JOURNAL OF VIROLOGY, Sept. 1980, p. 603-618
0022-538X/80/09-0613/16$02.00/0

Vol. 35, No. 3

Comparison of Epstein-Barr Virus Strains of Different Origin by Analysis of the Viral DNAs

G. W. BORNKAMM,[1]* H. DELIUS,[2] U. ZIMBER,[1] J. HUDEWENTZ,[1] AND M. A. EPSTEIN[3]

Institut für Virologie, Zentrum für Hygiene der Universität Freiburg, 7800 Freiburg,[1] and European Molecular Biology Laboratory, 6900 Heidelberg,[2] West Germany, and Department of Pathology, University of Bristol Medical School, Bristol, England[3]

Epstein-Barr virus (EBV) originating from Burkitt's lymphoma (P3HR-1 and CC34-5), nasopharyngeal carcinoma (M-ABA), transfusion mononucleosis (B95-8), and a patient with acute myeloblastic leukemia (QIMR-WIL) was isolated from virus-carrying lymphoid cell lines after induction with the tumor promoter 12-*O*-tetradecanoylphorbol-13-acetate. Viral DNA was analyzed by partial denaturation mapping and by use of the restriction endonucleases *Eco*RI, *Hin*dIII, and *Sal*I and separation of fragments in 0.4% agarose. By using the restriction enzyme data of B95-8 (EBV) and W91 (EBV) obtained by Given and Kieff (D. Given and E. Kieff, J. Virol. **28**:524-542, 1978), maps were established for the other virus strains. Comigrating fragments were assumed to be identical or closely related among the different strains. Fragments of different strains migrating differently were isolated, purified, radioactively labeled, and mapped by hybridization against blots of separated viral fragments. The results were as follows. (i) All strains studied were closely related. (ii) The number of internal repeats was variable among and within viral strains. (iii) B95-8 (EBV) was the only strain with a large deletion of about 12,000 base pairs at the right-hand side of the molecule. At the same site, small deletions of about 400 to 500 base pairs were observed in P3HR-1 (EBV) and M-ABA (EBV) DNA. (iv) P3HR-1 (EBV), the only nontransforming EBV strain, had a deletion of about 3,000 to 4,000 base pairs in the long unique region adjacent to the internal repeats carrying a *Hin*dIII site. (v) Small inserted sequences of 150 to 400 base pairs were observed in M-ABA (EBV) and B95-8 (EBV) at identical sites in the middle of the long unique region. (vi) Near this site, an insertion of about 1,000 base pairs was found in P3HR-1 (EBV) DNA. (vii) The cleavage patterns of P3HR-1 virus DNA and the results of blot hybridizations with P3HR-1 virus fragments are not conclusive and point to the possibility that in addition to the normal cleavage pattern some viral sequences may be arranged differently. Even though it is possible that small differences in the genome organization may have significant biological effects, the great similarity among different EBV strains does not favor the hypothesis that disease-specific subtypes exist.

Epstein-Barr virus (EBV) causes widespread inapparent infections in all human populations (9). In addition, the virus is known to be the etiological agent of infectious mononucleosis and is closely associated with two human malignant diseases, Burkitt's lymphoma and nasopharyngeal carcinoma (for a review, see references 10, 21, and 26). The great variability in the results of infection by the virus has raised the question as to whether different EBV strains may be responsible for the manifestation of infectious mononucleosis, Burkitt's lymphoma, and nasopharyngeal carcinoma. This paper is concerned with the comparison of EBV isolates from different sources.

Due to the lack of a permissive tissue culture system for propagation of the virus, only a limited number of isolates have been studied. Most of these isolates have been characterized in terms of their biological activity; biochemical analysis has been restricted to those strains which can be produced in sufficient quantity to purify the virus and the viral DNA. Most comparative studies on purified viral DNA have therefore been done with two strains, P3HR-1 (EBV) and B95-8 (EBV) (5, 19, 38, 41, 46), which differ in their biological properties (31) and more recently with the W91 strain (15, 39). P3HR-1 virus is produced by a human lymphoid cell line, which was derived by cloning from a Burkitt's lymphoma line (23); after the cloning, P3HR-1 virus gradually lost its transforming ability (31),

but showed the unique capacity to induce the early antigen complex upon superinfection of Raji cells (a nonproducer cell line of Burkitt's lymphoma origin [22]). In contrast, B95-8 virus, produced by a marmoset cell line transformed by an isolate originally derived from a patient with transfusion mononucleosis, is a transforming virus incapable of early antigen induction in Raji cells. P3HR-1 and B95-8 virus DNAs were shown to have deletions of about 12,000 base pairs at different positions of the genome (5), located in the *Eco*RI A and C fragments, respectively (39). Additionally, the P3HR-1 virus DNA was found to be heterogeneous by partial denaturation analysis. The heterogeneity of P3HR-1 virus DNA appears to be the reason for pronounced differences in the restriction enzyme patterns obtained by different laboratories (13, 19, 28, 41, 43, 46). The piece of DNA present in P3HR-1 (EBV) DNA and missing in the *Eco*RI C fragment of B95-8 (EBV) DNA was also found to be represented in the W91 strain, which is derived from a Burkitt's lymphoma (15, 39).

Apart from P3HR-1 virus, all other EBV isolates investigated, regardless of their origin, have been found to have transforming potential. These isolates include EBV from Burkitt's lymphomas either carried in cell lines derived directly from the tumors (11, 12, 34, 35) or obtained by transformation of marmoset cells after cocultivation with the lymphoma-derived lines (30). Other isolates have been obtained from malignant tumor cells of nasopharyngeal carcinoma by cocultivation of nude mouse-grown tumor fragments with human mononuclear cells of EBV-seronegative adults. Improvement of virus production could be obtained by passing the transforming virus to marmoset lymphocytes, resulting in the M-ABA line (3). Another source of EBV isolates has been human cell lines established from the peripheral blood of seropositive healthy individuals or patients with different diseases (7, 33, 36, 37).

Only some cell lines have provided enough virus after induction with the tumor promoter 12-*O*-tetradecanoylphorbol-13-acetate (24, 29, 49, 50) to allow an analysis of viral DNA. Thus, the DNAs of five strains (B95-8, CC34-5, P3HR-1, M-ABA, and QIMR-WIL) (3, 23, 30, 32, 37) were compared by partial denaturation mapping and by analysis of fragments after cleavage with restriction endonucleases.

Based on the linkage maps of B95-8 (EBV) and W91 (EBV) DNAs published by Given and Kieff (15), restriction enzyme maps were established for P3HR-1 (EBV), CC34-5 (EBV), QIMR-WIL (EBV), and M-ABA (EBV) DNAs. The latter seemed particularly interesting to us, since it represents the first isolate truly derived from tumor cells of a nasopharyngeal carcinoma. In contrast to the strains derived from EBV-associated diseases, the QIMR-WIL lymphoblastoid line was established from the peripheral blood of an Australian patient with myeloblastic leukemia (36) in the same way as isolations were performed from other seropositive individuals (7, 33).

MATERIALS AND METHODS

Cells. P3HR-1, B95-8, CC34-5, QIMR-WIL, and M-ABA cells were grown in RPMI 1640 (GIBCO Laboratories, Grand Island, N.Y.) with 10% fetal calf serum, 100 U of penicillin per ml, and 100 μg of streptomycin per ml. Cells were refed once weekly by replacing half of the medium. Initial cultures were obtained from G. Henle and W. Henle (P3HR-1), J. Pope (QIMR-WIL), and G. Miller (B95-8 and CC34-5). The virus produced by the CC34-5 line is presumably very similar to that produced by W91 cells (15), since the CC34-5 cell line was established by transformation with W91 (EBV). W91 is a marmoset line obtained by cocultivation with the human Burkitt's lymphoma line Nyevu (30). Establishment and properties of the M-ABA line have been described previously (3).

Virus and viral DNA. Induction of virus by 12-*O*-tetradecanoylphorbol-13-acetate and purification of virus and viral DNA were carried out as described previously (18). Briefly, cells were kept for 10 to 12 days with 20 ng of 12-*O*-tetradecanoylphorbol-13-acetate per ml and 0.1 to 1 μCi of [^{3}H]thymidine (Amersham Corp., Arlington Heights, Ill.) per ml. Cells were sedimented by low-speed centrifugation and suspended in 2 to 3 ml of distilled water. Virus was collected from the supernatant by centrifugation at 18,000 rpm at 4°C for 90 min in an R19 rotor (Beckman Instruments, Inc., Fullerton, Calif.). The pellet was suspended in virus standard buffer (10 mM Tris-hydrochloride [pH 7.4]–10 mM KCl–5 mM EDTA) by the aid of a Dounce homogenizer. The virus suspension was centrifuged for 60 min at 22,000 rpm at 4°C on a dextran T10 gradient (8) (5 to 30%, wt/vol) in an SW27 rotor (Beckman). The opalescent virus band was collected by puncturing the side of the tube and concentrated by another centrifugation at 22,000 rpm at 4°C in the SW27 rotor. The virus pellet was resuspended in virus standard buffer and stored at −70°C. Intracellular virus was isolated by homogenizing the cells, which had been suspended in water for 24 h at 4°C, in a Dounce homogenizer. Nuclei and cell debris were removed by low-speed centrifugation, and the supernatant was layered onto a dextran T10 gradient. Virus purified from 5 to 7 liters of culture fluid was lysed by addition of 0.1 volume of 10% (wt/vol) Sarkosyl NL and 100 μg of proteinase K per ml and incubated for 1 to 2 h at 37°C. CsCl and 10 mM Tris-hydrochloride (pH 7.4)–1 mM EDTA were added to give a final volume of about 10 ml and a final density of 1,705 g/ml. The DNA was centrifuged at 30,000 rpm at 23°C for 72 h in a 50 Ti rotor (Beckman). The DNA was collected from the bottom of the tube through a syringe needle (1.25 by 50 mm) at a restricted flow rate. Samples were pipetted into 4 ml of water and counted in a toluene–Triton X-100 (2:1)-based scintillator. Viral DNA was pooled, dialyzed against 10 mM Tris-

hydrochloride (pH 7.4)–1 mM EDTA, and stored at 0 to 4°C.

Partial denaturation of viral DNA. DNA was partially denatured in 6 M sodium perchlorate–10 mM sodium phosphate (pH 7.0)–1 mM EDTA in the presence of formaldehyde by incubating the sample for 30 to 60 min at 40°C as described previously (5). After the DNA was chilled in ice, salt and formaldehyde were removed on a small Sephadex G-100 column (3 by 0.2 cm), which was equilibrated with spreading buffer (0.1 M Tris-hydrochloride [pH 8.5]–10 mM EDTA–30% formamide). The DNA was eluted from the column with spreading buffer.

Preparation of DNA for electron microscopy. Cytochrome *c* (type V; Sigma Chemical Co., St. Louis, Mo.) was added to a final concentration of 100 μg/ml, and the DNA was spread on a 10% formamide hypophase (4). PM2 or T7 DNA or both were included as internal size markers, with molecular weights of 6.64×10^6 and 26.4×10^6, respectively (45).

Grids were stained with uranyl acetate, rotary shadowed with Pt-Pd, and examined in a Philips 301 electron microscope at 40 kV. Length measurements were made with the aid of a length-measuring device (Brühl L5) connected to a Wang 720C calculator. Orientation of the denaturation maps was achieved by visually correlating the most characteristic clusters of adenine-plus-thymine (A+T) and guanine-plus-cytosine (G+C) pairs. The scales of the histograms correspond to the lengths determined for native DNAs of the different strains.

Cleavage with restriction endonucleases and gel electrophoresis. The restriction enzymes *Eco*RI, *Hin*dIII, and *Sal*I were purchased from New England Biolabs, Beverly, Mass. Viral DNA was digested at 37°C for 2 to 3 h (*Eco*RI) or overnight in buffers indicated by New England Biolabs. After extraction with chloroform-isoamyl alcohol (24:1) and ethanol precipitation, samples were loaded onto 0.4% horizontal agarose gels in slots of 7-, 4.5-, 3-, or 1.5-mm width. Electrophoresis was carried out at 40 V for 12 to 18 h in buffer containing 36 mM Tris-hydroxide–30 mM sodium phosphate (pH 7.9)–1 mM EDTA and 0.5 μg of ethidium bromide per ml. Bands were visualized on a 254-nm transilluminator (UV Products, San Gabriel, Calif.) and photographed with a Polaroid camera with a Kodak wratten 23A filter. Fragments were transferred to nitrocellulose (Schleicher and Schüll, Dassel, West Germany) by the method of Southern (44) with modifications described by Botchan et al. (1).

Isolation of restriction enzyme fragments. For preparative isolation of fragments, 2 to 10 μg of digested DNA was loaded onto slots (14 to 35 by 1 mm) in 0.4% agarose gels. After separation of fragments, the gel was photographed on a 302-nm transilluminator (UV Products). As described by Tabak and Flavell (47), the gel was turned by 90° in the electrophoresis chamber, and the fragments were electrophoresed onto an adsorbent placed in front of the DNA fragments. The adsorbent hydroxyapatite or malachite green coupled to polyacrylamide (2, 27) (Boehringer, Mannheim, West Germany) was placed into small U-shaped pockets (of 6-mm width and 1.5-mm depth) covered on both sides with a nylon net. Fragments running closely together were separated by cutting the gel between the fragments, by moving them apart, and by filling new agarose into the space between them. All manipulations with the gel were controlled on the 302-nm transilluminator. After electrophoresis of the DNA onto the adsorbent, the pockets were removed from the gel, and the adsorbent was pipetted onto small Sephadex G-50 columns (5 by 0.35 cm) equilibrated with 10 mM Tris-hydrochloride (pH 7.4)–1 mM EDTA. DNA was eluted from hydroxyapatite with 0.5 M sodium phosphate (pH 6.8) and from malachite green coupled to polyacrylamide with 1 M sodium perchlorate–10 mM Tris-hydrochloride (pH 7.4)–1 mM EDTA in a total volume of 250 μl.

Labeling of viral DNA and DNA fragments. DNA and DNA fragments were labeled by nick translation with [^{32}P]TTP (Amersham Corp.; 300 to 400 Ci/mmol in a total volume of 50 to 100 μl by the procedure of Rigby et al. [40]. Non-incorporated triphosphates were removed on a Sephadex G-50 column.

Hybridization. Hybridization was carried out in polyethylene bags in a buffer containing 50% formamide, 3× SSC (1× SSC is 0.15 M sodium chloride plus 0.015 M sodium citrate), 0.02% bovine serum albumin, 0.02% polyvinylpyrrolidone, 0.02% Ficoll (6), 100 μg of denatured salmon sperm DNA per ml, and 1×10^5 to 5×10^5 cpm of heat-denatured labeled probe. The volume of the hybridization reaction was about 0.1 ml/cm^2. Hybridization was performed at 42 to 45°C for 3 to 4 days. Before hybridization, the filters were incubated for at least 2 h (usually overnight) at the same temperature and in the same solution without the labeled probe. Some experiments were done in 10% dextran sulfate (Pharmacia Fine Chemicals, Piscataway, N.J.) as described by Wahl et al. (48).

After hybridization, blots were washed four or five times in 2× SSC–0.5% sodium dodecyl sulfate at room temperature until no radioactivity could be detected in the washing fluid by a hand monitor. The blots were again sealed into polyethylene bags and incubated with shaking in 40 to 50 ml of 2× SSC–0.5% sodium dodecyl sulfate at 68°C for 1 to 2 h. After two or three additional washes at room temperature, the filters were washed briefly in water and air dried. Autoradiograms were made with a Kodak Royal X-omat film by using an intensifying screen (Du Pont Cronex Lightning-Plus).

RESULTS

Partial denaturation of QIMR-WIL (EBV), M-ABA (EBV), and CC34-5 (EBV). Viral DNA of the strains QIMR-WIL, CC34-5, and M-ABA was partially denatured at a neutral pH and low temperature in high concentrations of sodium perchlorate. After desalting, the molecules were spread in formamide and viewed in the electron microscope. The positions of loops representing A+T-rich areas were determined. The molecules were linearly aligned and oriented according to characteristic A+T- and G+C-rich areas.

Figure 1 shows the partial denaturation histograms of QIMR-WIL (EBV) DNA obtained from 16 molecules denatured to 37.2% and from

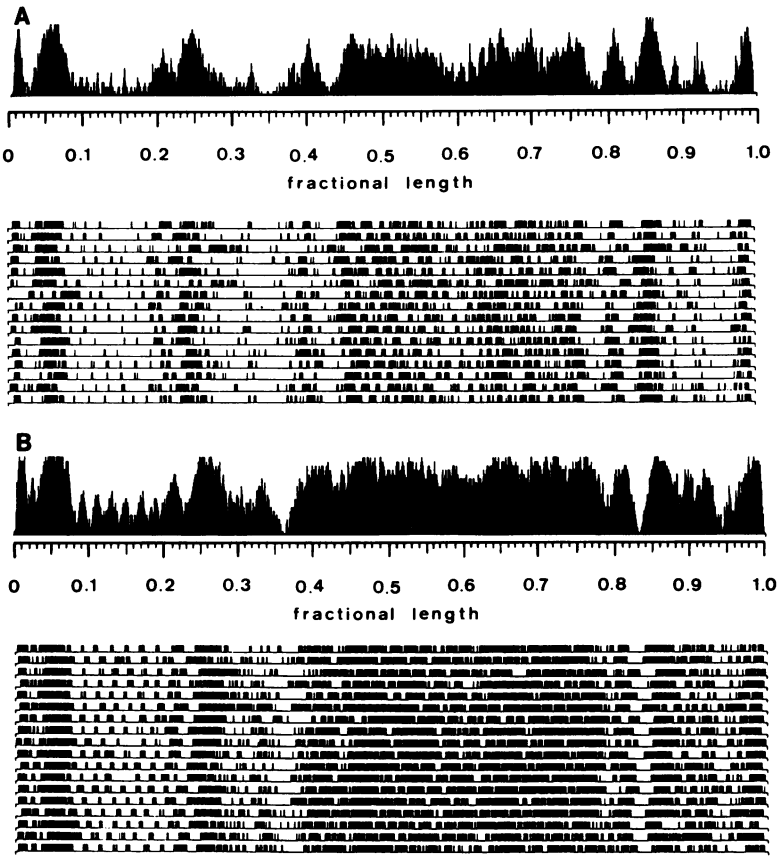

FIG. 1. *Partial denaturation histograms of QIMR-WIL (EBV) DNA compiled from 16 molecules denatured to 37.2 ± 2.1% (A) and from 18 molecules denatured to 66.1 ± 2.7% (B). Each line represents one molecule. Dark areas correspond to denatured parts of the molecules, and white areas correspond to native parts of the molecules. The maximal height corresponds to denaturation in 100% of the molecules.*

18 molecules denatured to 66.1%. Distinct regions of the molecules were preferentially denatured, resulting in a histogram with characteristic peaks at defined positions of the viral genome. At both ends, the distance from the terminus to the first denaturation loop varied among individual molecules, but was less pronounced than that observed earlier with P3HR-1 virus DNA. At the higher degree of denaturation, the fine structure of the histogram was lost within the A+T-rich areas; however, a row of peaks about 0.02 map unit apart from each other was observed in the G+C-rich part at the left-hand side of the molecule (0.08 to 0.2 fractional length), representing the internal repeats (16, 20, 41). Six small, evenly spaced peaks can be counted directly. One additional repeat may be hidden within the flanking A+T-rich sequences, resulting in a number of six or seven internal repeats in this virus strain. At the higher denaturation, two sites particularly rich in G+C were observed at positions 0.36 and 0.83, flanking the large A+T-rich area of the molecule (0.37 to 0.83 fractional length).

The partial denaturation maps of M-ABA (EBV) and CC34-5 (EBV) DNA molecules were very similar to those observed for QIMR-WIL (EBV). Therefore, the individual maps are not shown. The histograms obtained from the denaturation maps of both strains are shown in Fig. 2. The only difference clearly discernible is the number of internal repeats in the left part of the molecules. In the histogram of M-ABA (EBV), only four peaks corresponding to four to five repeats could be detected. In the denaturation maps of 16 individual M-ABA (EBV) DNA molecules, it became apparent that 4 of these molecules had a higher molecular weight by about 8×10^6 to 10×10^6 and contained four to five additional internal repeats. One molecule was observed with apparently only two or three internal repeats. In the case of CC34-5 (EBV)

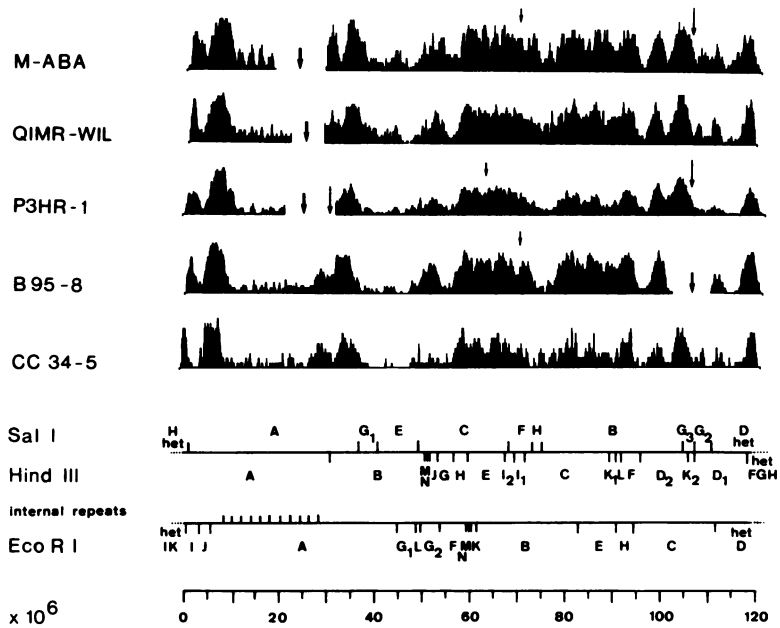

FIG. 2. *Partial denaturation histograms of M-ABA (EBV), QIMR-WIL (EBV), P3HR-1 (EBV) (5), B95-8 (EBV) (5), and CC34-5 (EBV) DNAs and EcoRI, SalI, and HindIII restriction endonuclease cleavage sites in CC34-5 (EBV) DNA. The restriction endonuclease data are taken from Given and Kieff (15) and are modified according to the data reported in this paper. The histograms are adjusted to the molecular weights determined for the DNAs of the different strains. Average denaturations were 40.4 ± 2.6% for M-ABA (EBV), 37.2 ± 2.1% for QIMR-WIL (EBV), 25.0 ± 3.0% for P3HR-1 (EBV), 33.8 ± 5.4% for B95-8 (EBV), and 20.7 ± 3.3% for CC34-5 (EBV) DNAs. The thick arrows and the long arrows point to large and small deletions, respectively; the short arrows point to sites of sequence insertions. Fragment HindIII-O is located either right or left of HindIII-I_1.*

DNA, the rate of denaturation was not sufficient to observe the repeats. The size of the undenatured area between the flanking A+T-rich parts suggests, however, that 10 internal repeats are present in this strain.

Comparison of the partial denaturation maps of QIMR-WIL (EBV), M-ABA (EBV), and CC34-5 (EBV) with those of B95-8 (EBV) and P3HR-1 (EBV). For a comparison of the denaturation histograms of the different viral strains, the molecular weights of the DNAs had to be determined. This determination was done in the electron microscope by a length comparison of viral DNAs of the five strains with the length of T7 DNA used as an internal size marker. The molecular weights thus obtained were as follows: (i) $121 \times 10^6 \pm 1.9\%$ for CC34-5 (EBV) DNA, (ii) $114 \times 10^6 \pm 2.1\%$ for B95-8 (EBV) DNA, (iii) $111 \times 10^6 \pm 2.5\%$ for QIMR-WIL (EBV) DNA, (iv) $110 \times 10^6 \pm 1.8\%$ for P3HR-1 (EBV) DNA, and (v) $109 \times 10^6 \pm 2.8\%$ for M-ABA (EBV) DNA. These values are somewhat higher than those published for P3HR-1 (EBV) and B95-8 (EBV) DNAs by Pritchett et al. (38). Our molecular weight estimate of B95-8 (EBV) DNA is, however, in good agreement with the revised value of Given and Kieff (16), obtained from a detailed restriction enzyme analysis. A few partially denatured molecules deviating significantly from these average lengths [as those M-ABA (EBV) DNA molecules described above with higher and lower numbers of internal repeats] were excluded from the construction of a histogram. The lengths of the histograms were adjusted to the molecular weights determined for the DNAs of the viral strains. The partial denaturation histograms of the DNAs of the different strains were aligned to each other, with gaps accounting for the differences in repeat units posed to the right side of the internal repeat region. Three factors introduce inaccuracies into the scale of the histograms. (i) The predominant number of terminal repeats may be different among different strains. Thus, a higher variation of the length of the terminus has been observed in the partial denaturation maps of P3HR-1 (EBV) DNA (5). (ii) The high standard deviation observed in the length measurements may not be due only to variations in the number of internal and terminal repeats (17, 25), but may also be due to nonproportional stretching along these molecules during the spreading procedure. (iii) Insertions or deletions which are too small to be detected by

partial denaturation analysis may be present in different strains. By analysis of restriction endonuclease fragments, it will be shown that such small insertions and deletions are indeed present in different viral strains.

With these reservations, a comparison of the denaturation histograms revealed the following. (i) The denaturation patterns of M-ABA (EBV), QIMR-WIL (EBV), and CC34-5 (EBV) did not show significant differences, apart from the variation in the number of internal repeats. (ii) Accordingly, the large deletion of 12,000 base pairs at the right-hand side of the B95-8 (EBV) genome was a unique feature of this virus strain. (iii) In the DNA preparations of B95-8 (EBV) and CC34-5 (EBV) studied here, the average number of internal repeats was identical. (iv) The region of the genome adjacent to the right-hand side of the internal repeats was characterized by an A+T-rich double peak in the histograms of all strains (0.19 to 0.23 and 0.23 to 0.28 fractional lengths in Fig. 1), except for P3HR-1 (EBV) DNA, in which a sequence of about 3,000 to 4,000 base pairs neighboring the internal repeats was deleted.

Comparison of the viral DNAs by use of restriction endonucleases. Partial denaturation analysis revealed that the DNAs of CC34-5 (EBV), QIMR-WIL (EBV), and M-ABA (EBV) are closely related and that QIMR-WIL (EBV) and M-ABA (EBV) contain the sequences present in P3HR-1 (EBV) and CC34-5 (EBV) which are missing in B95-8 virus DNA. Since partial denaturation mapping can reveal only major differences in the DNAs of viral strains, the DNAs of these strains were analyzed further on 0.4% agarose gels after digestion with restriction endonucleases. Analysis and mapping of the fragments were largely facilitated by the fact that linkage maps of *Eco*RI, *Hsu*I, and *Sal*I fragments of B95-8 (EBV) DNA were published by Given and Kieff (15). Since these data were available, the DNAs of the different strains were analyzed with the same endonucleases (the isoschizomer *Hin*dIII was used instead of *Hsu*I). It was assumed that fragments which comigrate with B95-8 (EBV) are identical or closely related and have the same map positions on the genome. Fragments migrating differently were isolated, purified by a second electrophoresis in agarose, labeled by nick translation with [^{32}P]TTP, and hybridized to blots of separated fragments to determine their positions on the genome. The nomenclature of Given and Kieff for the fragments of B95-8 (EBV) and W91 (EBV) DNAs was adopted. For the fragments of the other strains, including those of P3HR-1 (EBV), we attempted to apply the same nomenclature to corresponding fragments. It was not possible to follow this rule in all instances. Deviations were necessary, particularly in the cases of some large fragments [P3HR-1 (EBV) *Hin*dIII-A, -B, and -C; QIMR-WIL (EBV) *Hin*dIII-B and -C; P3HR-1 (EBV) and M-ABA (EBV) *Sal*I-A and -B]. Thus, the nomenclature of P3HR-1 (EBV) fragments used here does not follow any of the published reports (13, 19, 29, 41, 43, 46).

Cleavage with *Eco*RI. Figure 3a shows the fragment pattern of the DNAs of the virus strains P3HR-1, M-ABA, CC34-5, QIMR-WIL, and B95-8 after digestion with *Eco*RI and separation of the fragments. The patterns obtained from the different strains are obviously very similar. At the right, B95-8 (EBV) DNA fragments are labeled from A to N. At the left, P3HR-1 (EBV) DNA fragments are labeled accordingly. When the fragment patterns of the different strains are compared, the following observations can be made. (i) The size of the A fragments varies among different strains. In M-ABA (EBV) DNA, a faint band is visible above the fragment. (ii) The B and C fragments of CC34-5 (EBV) DNA may be separated if little DNA is loaded onto the gel. Under optimal conditions, the B and C bands of P3HR-1 (EBV) and less pronounced of M-ABA (EBV) can also be separated. The B and C bands of QIMR-WIL (EBV), however, were always found to be comigrating. (iii) In P3HR-1 (EBV) DNA, submolar bands with molecular weights of 14×10^6 to 18×10^6 (C′, C″, and C‴) are observed. These fragments are not found in all P3HR-1 virus DNA preparations. They apparently represent some of the fragments, giving rise to the confusion existing if one compares published P3HR-1 (EBV) DNA cleavage patterns (19, 29, 41, 43, 46). (iv) Another submolar fragment with a molecular weight of 10×10^6, probably representing part of the right terminus, is observed in P3HR-1 virus DNA. (v) The double molar fragment $G_{1,2}$ with a molecular weight of 4.2×10^6 is unimolar in P3HR-1 (EBV) DNA. (vi) The I fragment with a molecular weight of 2.7×10^6 is double molar in P3HR-1 (EBV) DNA. (vii) P3HR-1 (EBV) contains an additional fragment, J_2, with a molecular weight of 1.5×10^6. (viii) The K fragment of P3HR-1 (EBV) DNA migrates slightly faster than that of the other strains. (ix) The I fragment is missing in M-ABA (EBV). (x) The K fragment is absent from CC34-5 (EBV).

From the partial denaturation data, the variation in the size of the *Eco*RI A fragment can be easily explained by the different numbers of internal repeats present within the different strains. The larger size of the CC34-5 (EBV) B fragment and the missing K fragment could be due to the loss of a cleavage site between the

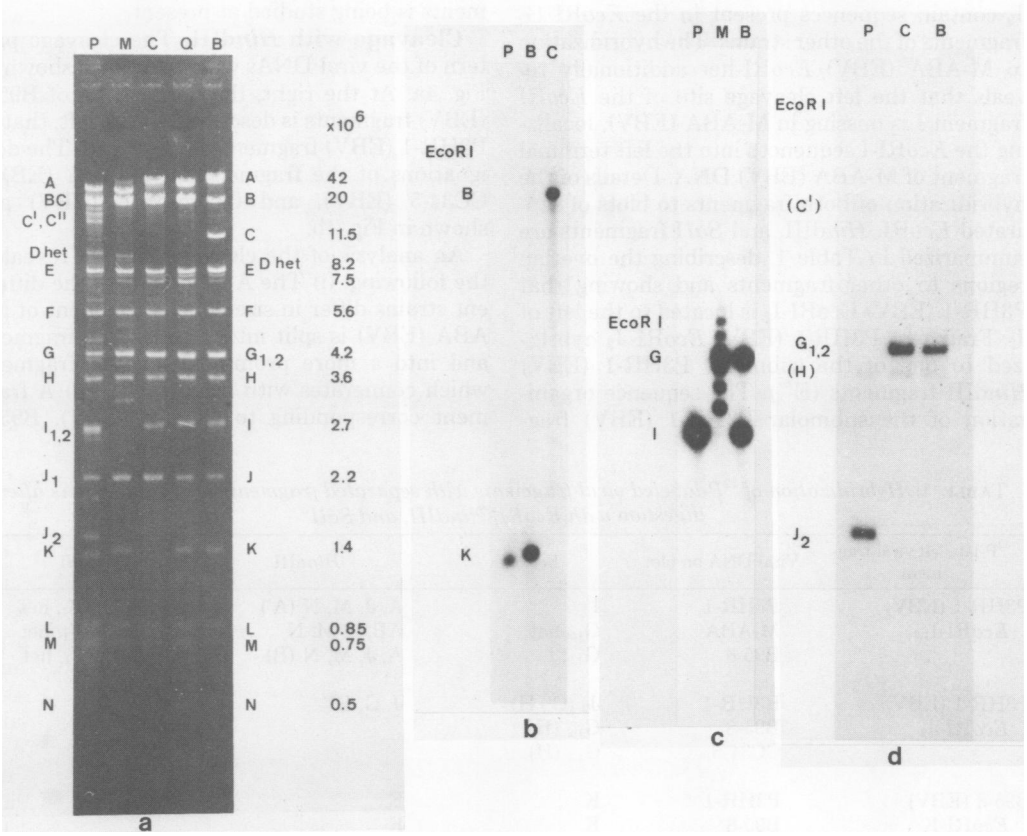

FIG. 3. *(a) Pattern of P3HR-1 (EBV) (P), M-ABA (EBV) (M), CC34-5 (EBV) (C), QIMR-WIL (EBV) (Q), and B95-8 (EBV) (B) DNA fragments after digestion with EcoRI and electrophoresis in 0.4% agarose. The molecular weights of the large fragments were taken from Given and Kieff (16). The molecular weights of fragments L, M, and N are only rough estimates, since molecular weight markers below 10^6 had not been included in the gel. (b, c, and d) Autoradiograms of blots of EcoRI fragments of P3HR-1 (EBV) (P), CC34-5 (EBV) (C), B95-8 (EBV) (B), and M-ABA (EBV) (M) DNAs after hybridization with ^{32}P-labeled fragments B95-8 (EBV) EcoRI-K (b), P3HR-1 (EBV) EcoRI-$I_{1,2}$ (c), and P3HR-1 (EBV) EcoRI-J_2 (d).*

neighboring K and B fragments. To test this, the B95-8 (EBV) K fragment was isolated, labeled in vitro with [^{32}P]TTP, and hybridized to blots containing CC34-5 virus DNA digested with *Eco*RI. As shown in Fig. 3b, the B95-8 (EBV) *Eco*RI K fragment hybridized to B95-8 (EBV) and P3HR-1 (EBV) K fragments and to CC34-5 (EBV) *Eco*RI-B.

The nature of the submolar bands of P3HR-1 (EBV) DNA not present in all P3HR-1 virus DNA preparations has not been fully elucidated and is the subject of a separate study. The appearance of two new fragments in P3HR-1 (EBV) DNA *Eco*RI-I_2 and -J_2 with a compiled molecular weight equaling that of the missing G_2 fragment suggested that P3HR-1 (EBV) contains an additional cleavage site in this fragment. To verify this assumption, P3HR-1 (EBV) *Eco*RI-J_2 and P3HR-1 (EBV) *Eco*RI-$I_{1,2}$ were isolated, labeled, and hybridized to blots containing separated *Eco*RI fragments of P3HR-1 (EBV), CC34-5 (EBV), and B95-8 (EBV). Figure 3c shows the result of the hybridization with P3HR-1 (EBV) *Eco*RI-J_2. It hybridized to P3HR-1 (EBV) *Eco*RI-J_2 and to CC34-5 (EBV) and B95-8 (EBV) *Eco*RI-$G_{1,2}$. In addition, a specific hybridization to *Eco*RI H fragments of all strains (or minor fragments migrating at the same position) and to P3HR-1 (EBV) *Eco*RI-C' was observed with prolonged exposure of the autoradiograms. The reason for this is not understood and is under investigation.

Hybridization with P3HR-1 (EBV) *Eco*RI-$I_{1,2}$ to blots containing separated *Eco*RI fragments of P3HR-1 (EBV), M-ABA (EBV), and B95-8 (EBV) revealed hybridization to P3HR-1 (EBV) *Eco*RI-$I_{1,2}$, to M-ABA (EBV) *Eco*RI-$G_{1,2}$ and *Eco*RI-het and to B95-8 (EBV) fragments *Eco*RI-I and -$G_{1,2}$ (Fig. 3d). This clearly indicates that the P3HR-1 (EBV) *Eco*RI fragments I_2 and

J_2 contain sequences present in the *Eco*RI G_2 fragments of the other strains. The hybridization to M-ABA (EBV) *Eco*RI-het additionally reveals that the left cleavage site of the *Eco*RI fragment I is missing in M-ABA (EBV), localizing the *Eco*RI-I sequences into the left terminal fragment of M-ABA (EBV) DNA. Details of the hybridization of both fragments to blots of separated *Eco*RI, *Hin*dIII, and *Sal*I fragments are summarized in Table 1, describing the overlap regions to other fragments and showing that P3HR-1 (EBV) EcoRI-I_2 is located to the left of J_2. Fragment P3HR-1 (EBV) *Eco*RI-J_2 hybridized to one of the submolar P3HR-1 (EBV) *Hin*dIII fragments (E‴). The sequence organization of the submolar P3HR-1 (EBV) fragments is being studied at present.

Cleavage with *Hin*dIII. The cleavage pattern of the viral DNAs with *Hin*dIII is shown in Fig. 4a. At the right, the designation of B95-8 (EBV) fragments is described; at the left, that of P3HR-1 (EBV) fragments is described. The designations of the fragments of M-ABA (EBV), CC34-5 (EBV), and QIMR-WIL (EBV) are shown in Fig. 4b.

An analysis of the cleavage pattern revealed the following. (i) The A fragments of the different strains differ in size. The A fragment of M-ABA (EBV) is split into a faint large fragment and into a more prominent smaller fragment which comigrates with fragment B. (ii) A fragment corresponding to CC34-5 (EBV), B95-8

TABLE 1. *Hybridization of ^{32}P-labeled viral fragments with separated fragments of various DNAs after digestion with EcoRI, HindIII, and SalI*[a]

^{32}P-labeled viral fragment	Viral DNA on blot	*Eco*RI	*Hin*dIII	*Sal*I
P3HR-1 (EBV)	P3HR-1	I	A, J, M, N (A')	B, D, G'$_1$, het
*Eco*RI-$I_{1,2}$	M-ABA	$G_{1,2}$ het	AB, J, M, N	D, C, G'$_1$, het
	B95-8	$G_{1,2}$, I	A, J, M, N (B)	A, C, G'$_1$, het
P3HR-1 (EBV)	B3HR-1	J_2 (C', H)	J, G, E‴	D
*Eco*RI-J_2	B95-8	$G_{1,2}$ (H)		
	CC34-5	$G_{1,2}$ (H)		
B95-8 (EBV)	P3HR-1	K	E	C
*Eco*RI-K	B95-8	K	E	C
	CC34-5	B	E	C
B95-8 (EBV)	P3HR-1	L	A	D
*Eco*RI-L	B95-8	L	B	C
B95-8 (EBV)	B95-8	M	E	C
*Eco*RI-M				
B95-8 (EBV)	P3HR-1	N	E, H	D
*Eco*RI-N	B95-8	N	E, H	D
QIMR-WIL (EBV)	P3HR-1	A	A	B, G_1, E
*Hin*dIII-C	B95-8	A	B	A, G_1, E
QIMR-WIL (EBV)	B95-8	$G_{1,2}$, L	B	E (B)
*Hin*dIII-E_2	QIMR-WIL		E_2	
QIMR-WIL (EBV)	P3HR-1	B	O	F
*Hin*dIII-O	B95-8	B	O	F
P3HR-1 (EBV)	P3HR-1	BC, F, K, M (D het)	E, H, I (G, C, E', E‴)	C (CD het)
*Sal*I-C	B95-8	B, F, K, M (C, D, het)	E, H, I (D, G)	C (D het)
P3HR-1 (EBV)	P3HR-1	F, I, J_2, L (G)	G, H, J, M, N, E‴ (A, A', B, C, D, E)	D (C, E)
*Sal*I-D	B95-8	F, $G_{1,2}$, L	G, J, M, N. (H, B, D)	C (D het, E)

[a] Fragments which hybridized weakly with the labeled probe are placed within parentheses.

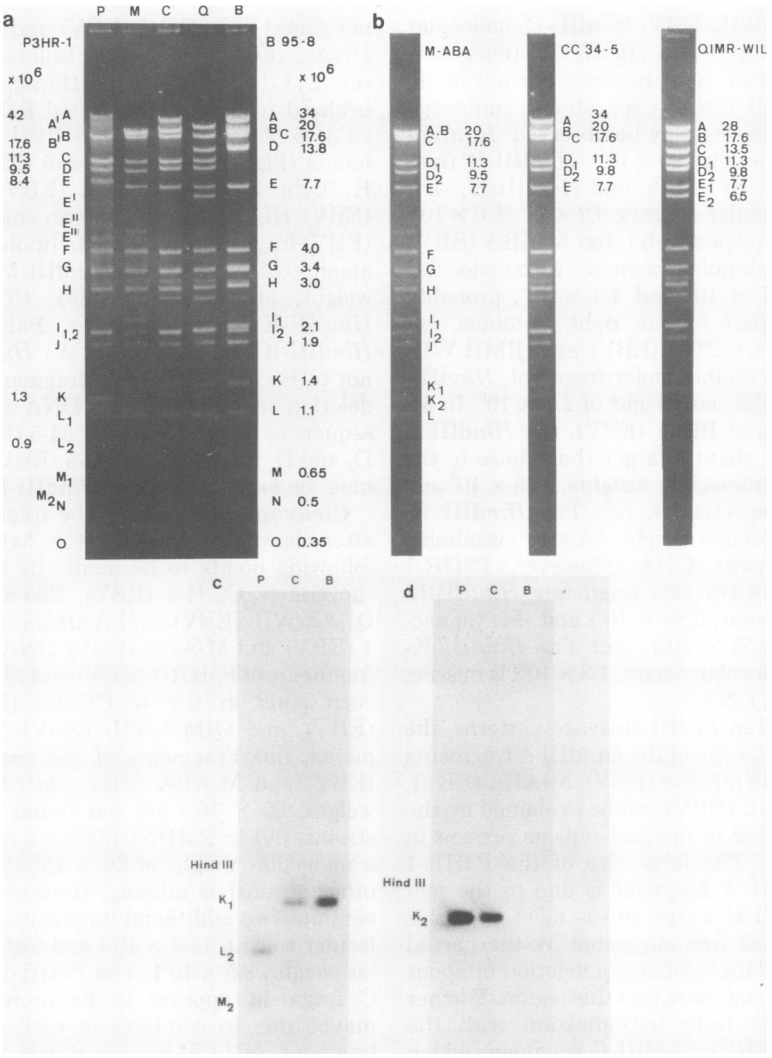

FIG. 4. *(a and b) Pattern of P3HR-1 (EBV) (P), M-ABA (EBV) (M), CC34-5 (EBV) (C), QIMR-WIL (EBV) (Q), and B95-8 (EBV) (B) DNA fragments after cleavage with HindIII and separation of fragments in 0.4% agarose. Designations and molecular weights of fragments are shown in (a) and (b). The three central lanes of (a) are shown separately in (b). The molecular weights of the large fragments were taken from Given and Kieff (16). Due to the lack of appropriate molecular weight markers, the molecular weights of fragments M, N, and O are only rough estimates. (c and d) Autoradiograms of blots containing separated HindIII fragments of P3HR-1 (EBV) (P), CC34-5 (EBV) (C), and B95-8 (EBV) (B) DNAs after hybridization with ^{32}P-labeled CC34-5 (EBV) HindIII fragments K_1 (c) and K_2 (d).*

(EBV), and M-ABA (EBV) *Hin*dIII-B (molecular weight, 20×10^6) is missing in P3HR-1 (EBV) and QIMR-WIL (EBV) DNAs. (iii) The *Hin*dIII B fragments of P3HR-1 (EBV) and QIMR-WIL (EBV) correspond to the *Hin*dIII C fragments of CC34-5 (EBV), B95-8 (EBV), and M-ABA (EBV) (molecular weight, 17.6×10^6). (iv) P3HR-1 (EBV) *Hin*dIII-C corresponds to *Hin*dIII-D_1 of CC34-5 (EBV), M-ABA (EBV), and QIMR-WIL (EBV). In some P3HR-1 virus DNA preparations, this fragment is double molar. (v) P3HR-1 (EBV) *Hin*dIII-D (molecular weight, 9.5×10^6) and M-ABA (EBV) *Hin*dIII-D_2 are slightly smaller than the corresponding fragments of CC34-5 (EBV) and QIMR-WIL (EBV) (molecular weight, 9.8×10^6). (vi) The *Hin*dIII E fragment of P3HR-1 (EBV) (molecular weight, 8.4×10^6) is significantly larger than the *Hin*dIII E fragments of the other strains (molecular weight, 7.7×10^6). (vii) QIMR-WIL (EBV), missing the fragment with a molecular weight of 20×10^6, contains two additional frag-

ments, QIMR-WIL (EBV) *Hin*dIII-C (molecular weight, 13.5×10^6) and *Hin*dIII-E_2 (molecular weight, 6.5×10^6). (viii) In some, but not in all, P3HR-1 (EBV) DNA preparations, additional submolar fragments may be observed: *Hin*dIII-A′ (molecular weight, 30×10^6), *Hin*dIII-B′ (molecular weight, 15×10^6), and *Hin*dIII-E′, -E″, and -E‴ (molecular weights, 6.2×10^6, 5.0×10^6, and 4.4×10^6, respectively). (ix) M-ABA (EBV) contains two submolar fragments with molecular weights of 4.7×10^6 and 4.3×10^6, probably representing part of the right terminus. (x) P3HR-1 (EBV), CC34-5 (EBV), and QIMR-WIL (EBV) have a double molar fragment, *Hin*dIII-$I_{1,2}$, with a molecular weight of 2.1×10^6. In M-ABA (EBV) and B95-8 (EBV), the *Hin*dIII I_1 fragments are slightly larger than those in the other strains (molecular weights, 2.35×10^6 and 2.2×10^6, respectively). (xi) The *Hin*dIII K_1 fragment (molecular weight, 1.4×10^6) is missing in P3HR-1 virus DNA. However, P3HR-1 (EBV) contains two new fragments, *Hin*dIII-L_2 (molecular weight, 0.85×10^6) and -M_2 (molecular weight, 0.55×10^6). (xii) The *Hin*dIII K_2 fragment (molecular weight, 1.3×10^6) is missing in B95-8 virus DNA.

As observed in *Eco*RI cleavage patterns, the variability in the size of the *Hin*dIII A fragments of CC34-5 (EBV), B95-8 (EBV), M-ABA (EBV), and QIMR-WIL (EBV) can be explained by the different number of internal repeats present in this fragment. The large size of the P3HR-1 (EBV) *Hin*dIII A fragment is due to the fact that a *Hin*dIII cleavage site is deleted in this strain. This was first suggested by the partial denaturation data localizing a deletion of about 3,000 to 4,000 base pairs into this region. Further evidence came from hybridization with the QIMR-WIL (EBV) *Hin*dIII C fragment, which hybridized to B95-8 (EBV) *Hin*dIII-B and to P3HR-1 (EBV) *Hin*dIII-A (Table 1). QIMR-WIL (EBV) *Hin*dIII-E_2 hybridized also to B95-8 (EBV) *Hin*dIII-B, indicating that the QIMR-WIL (EBV) C and E_2 fragments correspond to the *Hin*dIII B fragments of B95-8 (EBV), CC34-5 (EBV), and M-ABA (EBV). The results of the hybridization with both fragments are summarized in Table 1 (autoradiograms not shown), locating QIMR-WIL (EBV) *Hin*dIII-E_2 to the right of *Hin*dIII-C and determining the overlaps to other fragments.

The nature of the submolar P3HR-1 (EBV) fragments A′, B′, E′, E″, and E‴ is not understood and is presently under investigation. The size difference between the *Hin*dIII D and D_2, *Hin*dIII E, and *Hin*dIII I fragments of the different strains was studied in more detail and will be described below.

The *Hin*dIII K_1 and K_2 fragments, which were not found in P3HR-1 (EBV) and B95-8 (EBV) DNAs, respectively, were isolated from separated CC34-5 (EBV) *Hin*dIII fragments and hybridized to blots of separated P3HR-1 (EBV), CC34-5 (EBV), and B95-8 (EBV) *Hin*dIII fragments (Fig. 4c and d). CC34-5 (EBV) *Hin*dIII-K_1 hybridized to CC34-5 (EBV) and B95-8 (EBV) *Hin*dIII-K_1 and to two smaller P3HR-1 (EBV) fragments, *Hin*dIII-L_2 (molecular weight, about 0.85×10^6) and *Hin*dIII-M_2 (molecular weight, about 0.55×10^6). CC34-5 (EBV) *Hin*dIII-K_2 hybridized to P3HR-1 (EBV) *Hin*dIII-K and CC34-5 (EBV) *Hin*dIII-K_2, but not to B95-8 (EBV) DNA fragments. Since the deletion in B95-8 (EBV) DNA is flanked by sequences present in the CC34-5 (EBV) *Hin*dIII D_1 and D_2 fragments, CC34-5 (EBV) *Hin*dIII-K_2 must be located between *Hin*dIII-D_1 and -D_2.

Cleavage with *Sal*I. The fragment pattern after cleavage with *Sal*I (Fig. 5a) permits the following points to be made. (i) Fragments of the size of CC34-5 (EBV), B95-8 (EBV), and QIMR-WIL (EBV) *Sal*I-A are missing in P3HR-1 (EBV) and M-ABA (EBV) DNAs. (ii) *Sal*I A fragments of P3HR-1 (EBV) and M-ABA (EBV) correspond in size to CC34-5 (EBV), B95-8 (EBV), and QIMR-WIL (EBV) *Sal*I B fragments. (iii) Fragments of the size of P3HR-1 (EBV) and M-ABA (EBV) *Sal*I-B (molecular weight, 22×10^6) are not found in the other strains. (iv) In P3HR-1 (EBV), a fragment with a molecular weight of 20×10^6 (*Sal*I-C of the other strains) is missing. However, this strain contains two additional fragments, *Sal*I-C (molecular weight, 11.5×10^6) and *Sal*I-D (molecular weight, 8.5×10^6). The P3HR-1 (EBV) *Sal*I C fragment appears to be more prominent, maybe due to comigration with the terminal fragment *Sal*I-CD het. (v) P3HR-1 (EBV) contains a set of submolar fragments in the range between molecular weights of 6×10^6 and 22×10^6. (vi) Terminal fragments *Sal*I-D het are somewhat smaller in CC34-5 (EBV) and QIMR-WIL (EBV) DNAs than they are in the other strains. (vii) The *Sal*I F fragments of M-ABA (EBV) (molecular weight, 5.2×10^6) and B95-8 (EBV) (molecular weight, 5.1×10^6) are somewhat larger than the corresponding *Sal*I F fragments of the other strains (molecular weight, 5.0×10^6). (viii) Fragments *Sal*I-G_2 and -G_3 are missing in B95-8 virus DNA.

Starting with the description of the large fragments, it was obvious that all strains contain a fragment with a molecular weight of 22×10^6 [*Sal*I-B of CC34-5 (EBV), B95-8 (EBV), and QIMR-WIL (EBV) and *Sal*I-A of P3HR-1 (EBV) and M-ABA (EBV)], with presumably corresponding sequences. If so, it had to be assumed that the sequences present in *Sal*I-A

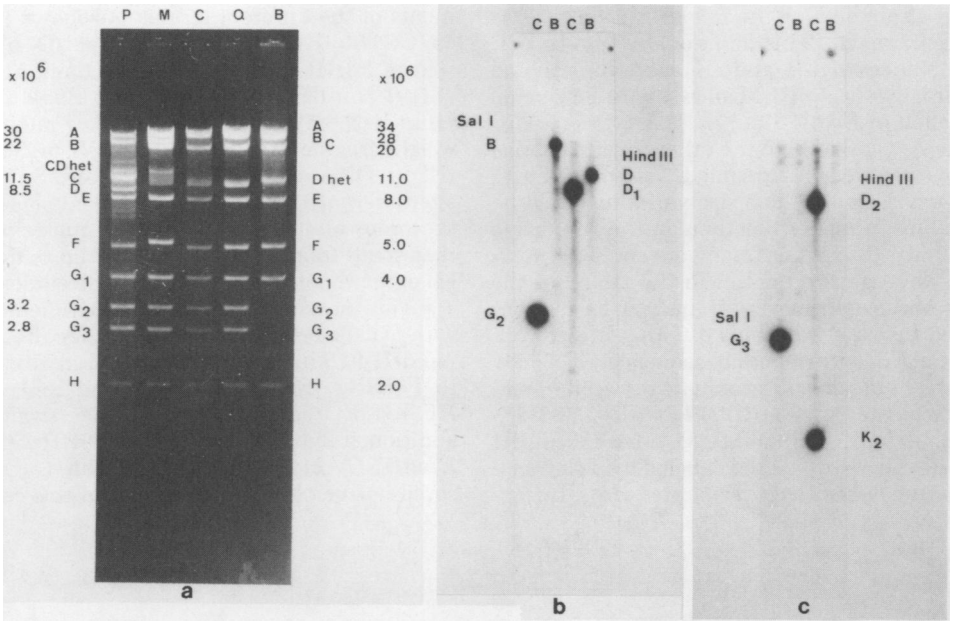

FIG. 5. *(a) Pattern of P3HR-1 (EBV) (P), M-ABA (EBV) (M), CC34-5 (EBV) (C), QIMR-WIL (EBV) (Q), and B95-8 (EBV) (B) DNA fragments after cleavage with SalI and separation of fragments in 0.4% agarose. Designations and molecular weights are given for P3HR-1 (EBV) fragments at the left side and for B95-8 (EBV) DNA fragments at the right side. (b and c) Autoradiograms of blots containing separated SalI (left lanes) and HindIII fragments (right lanes) of CC34-5 (EBV) (C) and B95-8 (EBV) (B) DNAs after hybridization with ^{32}P-labeled CC34-5 (EBV) SalI-G_2 (b) and CC34-5 (EBV) SalI-G_3 (c).*

of CC34-5 (EBV), B95-8 (EBV), and QIMR-WIL (EBV) would be located in *Sal*I-B of P3HR-1 (EBV) and M-ABA (EBV). To test this, P3HR-1 (EBV) fragments *Sal*I-A and -B were isolated and redigested with *Bgl*II. The cleavage pattern revealed that P3HR-1 (EBV) *Sal*I-B contains the internal repeats, thus locating this fragment to the left-hand side of the P3HR-1 (EBV) genome (data not shown).

Hybridization with labeled P3HR-1 (EBV) fragments *Sal*I-C and -D revealed that homologous sequences are represented in B95-8 (EBV) *Sal*I-C. Details of the hybridization are given in Table 1, providing evidence that P3HR-1 (EBV) *Sal*I-D is located to the left of P3HR-1 (EBV) *Sal*I-C. Hybridization of P3HR-1 (EBV) *Sal*I-D to P3HR-1 (EBV) *Hin*dIII-E''' cannot be interpreted at present and may point to sequence rearrangements within the P3HR-1 (EBV) genome. Both fragments, P3HR-1 (EBV) *Sal*I-C and -D, hybridized weakly to a number of other fragments (Table 1), probably due to cross contamination and to contamination with the right terminal fragment *Sal*I-CD het.

The submolar P3HR-1 (EBV) fragments probably belong in part to the terminal fragment *Sal*I-CD het. However, their nature is not fully established. CC34-5 (EBV) fragments *Sal*I-G_2 and -G_3, missing in B95-8 virus DNA, were isolated, labeled, and hybridized to blots of separated CC34-5 (EBV) and B95-8 (EBV) *Sal*I and *Hin*dIII fragments. As shown in Fig. 5b and c, CC34-5 (EBV) *Sal*I-G_2 hybridized to CC34-5 (EBV) *Sal*I-G_2 and *Hin*dIII-D_1 and only weakly to B95-8 (EBV) *Sal*I-B and *Hin*dIII-D. CC34-5 (EBV) *Sal*I-G_3 hybridized to CC34-5 (EBV) *Sal*I-G_3 and to *Hin*dIII-D_2 and -K_2, but not at all to B95-8 (EBV) DNA fragments. From the intensity of hybridization of CC34-5 (EBV) *Sal*I-G_2 to B95-8 (EBV) fragments, it may be estimated that about 15 to 25% of the sequences of the right side of the *Sal*I G_2 fragment are represented in the B95-8 (EBV) *Sal*I B fragment.

The differences in the sizes of the *Sal*I F fragments of the different strains were studied in more detail and are described below.

Deletions and insertions. As described above, some fragments of the different strains differ in size (Fig. 3a, 4a, and 5a). Besides those carrying the internal or terminal repeats, size variations were observed in the following fragments: *Eco*RI-B, *Hin*dIII-D_2 [corresponding to P3HR-1 (EBV) *Hin*dIII-D], *Eco*RI-K, *Hin*dIII-E, *Hin*dIII-I_1, and *Sal*I-F. The larger size of the *Eco*RI B fragment of CC34-5 (EBV) was explained by the fact that a cleavage site is missing

in this strain, linking the *Eco*RI-K sequences to the B fragment. This additionally proves that fragments *Eco*RI-B and -K are adjacent and that fragments *Eco*RI-M and -N must be located to the left of *Eco*RI-K.

The size variation in the other fragments was, however, less easily explained. Two possibilities were envisaged. (i) The size variation could be due to insertions or deletions in the respective fragments. (ii) Larger fragments could be missing a cleavage site present in the DNAs of the other strains. Primarily, it had to be demonstrated that the fragments differing in size contain, indeed, corresponding sequences. To show this and to possibly discriminate between (i) and (ii) above, the CC34-5 (EBV) *Hin*dIII D_2, P3HR-1 (EBV) *Hin*dIII E, and M-ABA (EBV) *Hin*dIII I_1 fragments were isolated, labeled by nick translation, and hybridized to separated *Hin*dIII fragments of the different strains. As shown in Fig. 6a, CC34-5 (EBV) *Hin*dIII fragment D_2 hybridized to P3HR-1 (EBV) *Hin*dIII-D and M-ABA (EBV) *Hin*dIII-D_2 and weakly to B95-8 (EBV) *Hin*dIII-D. Hybridization to a low-molecular-weight fragment of P3HR-1 (EBV) or M-ABA (EBV) DNA could not be observed. Since the size difference between the fragments is only in the order of 400 base pairs, it is quite possible that small fragments could have run out of the gel or were not transferred to nitrocellulose.

Figure 6b shows the same experiment done with labeled P3HR-1 virus DNA fragment *Hin*dIII-E. This fragment hybridized efficiently to P3HR-1 (EBV) *Hin*dIII-E and less to the *Hin*dIII E fragments of the other strains. In addition, it hybridized weakly to P3HR-1 (EBV) *Hin*dIII-E′. Hybridization to small fragments could not be observed, although in this case an

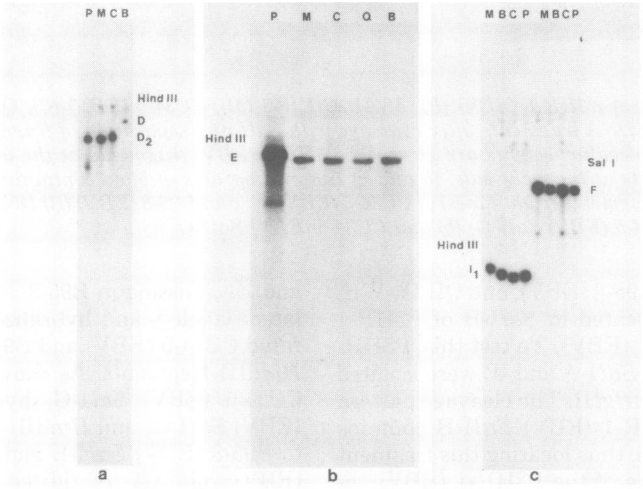

FIG. 6. *(a, b, and c) Autoradiograms of blots containing separated HindIII [(a), (b), and the left four lanes in (c)] and SalI [the right four lanes in (c)] DNA fragments of P3HR-1 (EBV) (P), M-ABA (EBV) (M), CC34-5 (EBV) (C), QIMR-WIL (EBV) (Q), and B95-8 (EBV) (B) after hybridization with ^{32}P-labeled CC34-5 (EBV) HindIII-D_2 (a), P3HR-1 (EBV) HindIII-E (b), and M-ABA (EBV) HindIII-I_1 (c).*

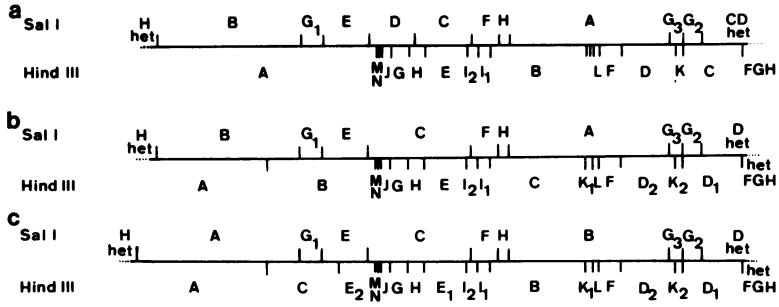

FIG. 7. *HindIII and SalI restriction endonuclease cleavage sites in P3HR-1 (EBV) (a), M-ABA (EBV) (b), and QIMR-WIL (EBV) (c) DNAs. Fragment HindIII-O is located either right or left of HindIII-I_1. The extra bands in P3HR-1 (EBV) DNA (see text) are not represented.*

additional fragment of about 1,000 base pairs would have been detected.

Hybridization with labeled M-ABA (EBV) *Hin*dIII-I_1 to separated *Hin*dIII and *Sal*I fragments is shown in Fig. 6c. Apparently, this fragment hybridized only to the *Hin*dIII I_1 and *Sal*I F fragments of the different strains. Since in the same area of the genome the same size variations were observed in fragments generated by two different restriction endonucleases, it may be concluded that M-ABA (EBV) and B95-8 virus DNAs have insertions of about 150 and 400 base pairs, respectively, at the same position of the genome or very nearby.

DISCUSSION

Five different EBV strains carried by lymphoid cell lines and originating from Burkitt's lymphoma (P3HR-1 and CC34-5), nasopharyngeal carcinoma (M-ABA), transfusion mononucleosis (B95-8), and a patient with myeloblastic leukemia (QIMR-WIL) were compared by partial denaturation mapping and analysis of restriction endonuclease fragments. Besides the deletion of about 12,000 base pairs at the right-hand side of the B95-8 (EBV) DNA molecule, which has been reported previously (5, 15, 39), only small differences were observed in the partial denaturation patterns. The main difference was found in the number of internal repeat units, varying from an average of 4 to 5 in M-ABA to about 10 in B95-8 (EBV) and CC34-5 (EBV). Adjacent to the internal repeats, sequences of about 3,000 to 4,000 base pairs carrying a *Hin*dIII site are missing in the P3HR-1 strain. The proper location of this deletion has only been detected by comparison of the denaturation histograms of several virus strains and not in our earlier study. That sequences are missing in this part of the genome in P3HR-1 (EBV) DNA has also been reported by Raab-Traub et al. (39) after hybridization of a B95-8 virus-specific probe, from which all sequences homologous to P3HR-1 virus DNA had been removed, to the B95-8 (EBV) *Eco*RI A and *Hsu*I B fragments.

Concerning the deletion of about 12,000 base pairs at the right-hand side of the B95-8 (EBV) genome, it was particularly interesting to determine whether the extra piece of DNA already known to be present in P3HR-1 (EBV) and CC34-5 (EBV) would be represented in the two virus strains, M-ABA and QIMR-WIL, of different geographical and pathological origin. Obviously, these strains contain the "extra" DNA, indicating that the large deletion in B95-8 (EBV) is the exception rather than the rule. No further differences were observed in the partial denaturation histograms of the different strains. Partial denaturation mapping, however, allows only the detection of major differences in the organization of the genome. To allow a more detailed study of the different strains, viral DNA was analyzed after digestion with the restriction endonucleases *Eco*RI, *Hin*dIII, and *Sal*I. Based on the linkage maps provided for B95-8 (EBV) and W91 (EBV) by Given and Kieff (15), maps were established for CC34-5 (EBV), M-ABA (EBV), QIMR-WIL (EBV), and P3HR-1 (EBV) DNAs (Fig. 7), revealing insertions or deletions in the different strains which had not been detected by partial denaturation analysis. Thus, insertions of about 150 and 400 base pairs were identified in the *Hin*dIII I_1 fragment of B95-8 (EBV) and M-ABA (EBV) DNAs, respectively. Another site of variability was found in the *Hin*dIII D_2 fragment, which corresponds to P3HR-1 (EBV) *Hin*dIII-D. Most of the sequences of this fragment are missing in B95-8 virus DNA (15, 39). In P3HR-1 (EBV) and M-ABA (EBV) DNAs, this fragment is about 400 to 500 base pairs smaller than the corresponding CC34-5 (EBV) and QIMR-WIL (EBV) fragments. This also suggests that in P3HR-1 (EBV) and M-ABA (EBV) DNAs small deletions are located at this site of the genome. This site has also been identified as the major site of sequence variability by Rymo et al. (42) in an analysis of the intracellular EBV DNA from tumors and cell lines after cleavage with *Eco*RI and transfer to nitrocellulose filters.

Another variation among the different strains was found in the *Hin*dIII E fragments. The P3HR-1 (EBV) *Hin*dIII E fragment is about 1,000 base pairs larger than the corresponding fragments of the other strains. The possibility that a *Hin*dIII site was lost in P3HR-1 virus DNA, generating a larger *Hin*dIII E fragment, was excluded, since P3HR-1 (EBV) *Hin*dIII-E hybridized exclusively to the *Hin*dIII E fragments of the other strains. It is presently not possible to decide whether this fragment contains sequences unique to the P3HR-1 virus strain or repetitions of sequences, which are also represented in the DNAs of the other strains.

The P3HR-1 strain appears to be exceptional in many respects. As is well known, P3HR-1 virus is the only EBV strain which is incapable of transforming human B lymphocytes (31). However, it has the ability to induce an abortive cycle in EBV genome-carrying nonproducer cells (22, 31). The structural organization of the P3HR-1 virus genome turned out to be difficult to characterize. Reports of several laboratories on the cleavage pattern of P3HR-1 (EBV) DNA after digestion with *Eco*RI (19, 28, 41, 43, 46) and *Hin*dIII (13, 19, 28, 41) revealed discordant data, although all reports on B95-8 virus DNA were in good agreement (19, 41, 46). In addition,

the partial denaturation pattern of P3HR-1 virus DNA (5) and biological experiments on EBV-determined nuclear antigen and EA induction suggested heterogeneity of the P3HR-1 virus (14). Again, in this study, the structural organization of the P3HR-1 virus genome is not fully elucidated. The majority of fragments could be aligned to a linkage map (Fig. 7a), resembling that of the other strains, with two differences characteristic for the P3HR-1 strain: a deletion of about 3,000 to 4,000 base pairs in the long unique region adjacent to the internal repeats and an insertion of about 1,000 base pairs in the *Hin*dIII E fragment. It is suggestive to correlate these structural peculiarities with biological functions of the virus. Thus, the sequences neighboring the internal repeats which are deleted in the P3HR-1 strain could play an important role in the transformation of B lymphocytes. This is supported further by the observation of Fresen et al. (13; K. O. Fresen, M.-S. Cho, and H. zur Hausen, *in Cold Spring Harbor Conference on Cell Proliferation*, in press) with recombinant EBV strains obtained by rescue of resident genomes from nonproducer cells by superinfection with P3HR-1 virus. All recombinants studied so far have transforming capacity and contain the piece of DNA deleted in P3HR-1 virus.

Although the linkage map for the P3HR-1 strain was established by analogy to the other strains, a number of fragments do not fit into this pattern. Their occurrence varies with different preparations, thus giving rise to the discrepancies in the different reports on P3HR-1 virus DNA cleavage products. P3HR-1 (EBV) *Sal*I-D and P3HR-1 (EBV) *Eco*RI-J_2 hybridized to some of these fragments, indicating that sequence rearrangements may have taken place during the synthesis of P3HR-1 virus DNA. The appearance of some fragments in more than molar amounts [P3HR-1 (EBV) *Hin*dIII-C and -K and also P3HR-1 (EBV) *Sal*I-G_2 and -G_3] suggests that the right terminus of the molecule may additionally be overrepresented in some P3HR-1 virus DNA preparations. No information is presently available as to whether sequences present in the extra bands of P3HR-1 virus DNA are represented in the genome of the other strains.

It is not known whether this type of sequence heterogeneity in P3HR-1 virus plays a role in the expression of biological functions, e.g., EA inductions in Raji cells. Interestingly, the extra bands of P3HR-1 virus DNA, which do not fit into the linkage map, are preferentially replicated in superinfected Raji cells (M.-S. Cho, K. O. Fresen, and H. zur Hausen, Int. J. Cancer, in press). An analysis of the sequence arrangements in the extra bands of P3HR-1 virus DNA is in progress.

With the exception of the P3HR-1 virus, the great similarity of the strains studied here is striking. The three isolated strains CC34-5, M-ABA, and QIMR-WIL originated not only from patients with different diseases but also from different geographical areas. Only minor differences could be detected among their DNAs. Even though it is possible that small differences the genome organization may have significant biological effects, the great similarity among these strains does not favor the hypothesis that disease-specific subtypes of EBV exist.

ACKNOWLEDGMENTS

We thank George Miller for providing CC34-5 cells and H. zur Hausen and K. O. Fresen for critically reading the manuscript.

This work was supported by Die Deutsche Forschungsgemeinschaft (SFB 31).

LITERATURE CITED

1. **Botchan, M., W. Topp, and J. Sambrook.** 1976. The arrangement of simian virus 40 sequences in the DNA of transformed cells. Cell **9**:269-287.
2. **Bünemann, H., and W. Müller.** 1978. Base specific fractionation of double stranded DNA: affinity chromatography on a novel type of adsorbent. Nucleic Acids Res. **5**:1059-1074.
3. **Crawford, D. H., M. A. Epstein, G. W. Bronkamm, B. G. Achong, S. Finerty, and J. L. Thompson.** 1979. Biological and biochemical observations on isolates of EB virus from the malignant epithelial cells of two nasopharyngeal carcinomas. Int. J. Cancer. **24**:294-302.
4. **Davis, R. W., M. Simon, and N. Davidson.** 1971. Electron microscopy heteroduplex methods for mapping regions of base sequence homology in nucleic acids. Methods Enzymol. **21**:413-482.
5. **Delius, H., and G. W. Bornkamm.** 1978. Heterogeneity of Epstein-Barr virus. III. Comparison of a transforming and a nontransforming virus by partial denaturation mapping of their DNAs. J. Virol. **27**:81-89.
6. **Denhardt, D. T.** 1966. A membrane filter technique for the detection of complementary DNA. Biochem. Biophys. Res. Commun. **23**:641-646.
7. **Diehl, V., G. Henle, W. Henle, and G. Kohn.** 1968. Demonstration of a herpes group virus in cultures of peripheral leukocytes from patients with infectious mononucleosis. J. Virol. **2**:663-669.
8. **Dolyniuk, M., R. Pritchett, and E. Kieff.** 1976. Proteins of Epstein-Barr virus. I. Analysis of the polypeptides of purified enveloped Epstein-Barr virus. J. Virol. **17**:935-949.
9. **Epstein, M. A., and B. G. Achong.** 1979. Introduction: discovery and general biology of the virus, p. 1-22. *In* M. A. Epstein and B. G. Achong (ed.), The Epstein-Barr virus. Springer Verlag, Berlin.
10. **Epstein, M. A., and B. G. Achong.** 1979. The relationship of the virus to Burkitt's lymphoma, p. 23-38. *In* M. A. Epstein and B. G. Achong (ed.), The Epstein-Barr virus. Springer Verlag, Berlin.
11. **Epstein, M. A., and Y. M. Barr.** 1965. Characteristics and mode of growth of a tissue culture strain (EB1) of human lymphoblasts from Burkitt's lymphoma. J. Natl. Cancer Inst. **34**:231-240.
12. **Epstein, M. A., G. Henle, B. G. Achong, and Y. M.**

Barr. 1965. Morphological and biological studies on a virus in cultured lymphoblasts from Burkitt's lymphoma. J. Exp. Med. **121**:761-770.

13. **Fresen, K. O., M.-S. Cho, L. Gissmann, and H. zur Hausen.** 1979. NC 37-R1 EB-virus: a possible recombinant between intracellular NC 37 viral DNA and superinfecting P3HR-1 EBV. Intervirology **12**:303-310.
14. **Fresen, K. O., and H. zur Hausen.** 1976. Establishment of EBNA-expressing cell lines by infection of Epstein-Barr virus (EBV)-genome-negative human lymphoma cells with different EBV strains. Int. J. Cancer **17**:161-166.
15. **Given, D., and E. Kieff.** 1978. DNA of Epstein-Barr virus. IV. Linkage map of restriction enzyme fragments of the B95-8 and W91 strains of Epstein-Barr virus. J. Virol. **28**:524-542.
16. **Given, D., and E. Kieff.** 1979. DNA of Epstein-Barr virus. VI. Mapping of the internal tandem reiteration. J. Virol. **31**:315-324.
17. **Given, D., D. Yee, K. Griem, and E. Kieff.** 1979. DNA of Epstein-Barr virus. V. Direct repeats of the ends of Epstein-Barr virus DNA. J. Virol. **30**:852-862.
18. **Graessmann, A., H. Wolf, and G. W. Bornkamm.** 1980. Expression of Epstein-Barr virus genes in different cell types after microinjection of viral DNA. Proc. Natl. Acad. Sci. U.S.A. **77**:433-436.
19. **Hayward, S. D., and E. Kieff.** 1977. DNA of Epstein-Barr virus. II. Comparison of the molecular weights of restriction endonuclease fragments of the DNA of Epstein-Barr virus strains and identification of end fragments of the B95-8 strain. J. Virol. **23**:421-429.
20. **Hayward, S. D., L. Nogee, and G. S. Hayward.** 1980. Organization of repeated regions within the Epstein-Barr virus DNA molecule. J. Virol. **33**:507-521.
21. **Henle, G., and W. Henle.** 1979. The virus as the etiological agent of infectious mononucleosis, p. 297-320. *In* M. A. Epstein and B. G. Achong (ed.), The Epstein-Barr virus. Springer Verlag, Berlin.
22. **Henle, W., G. Henle, B. A. Zajac, G. Pearson, R. Waubke, and M. Scriba.** 1970. Differential reactivity of human serums with early antigens induced by Epstein-Barr virus. Science **169**:188-190.
23. **Hinuma, Y., M. Kohn, J. Yamaguchi, D. J. Wudarski, J. R. Blakeslee, Jr., and J. T. Grace, Jr.** 1967. Immunofluorescence and herpes-type virus particles in the P3HR-1 Burkitt lymphoma cell line. J. Virol. **1**: 1045-1051.
24. **Hudewentz, J., G. W. Bornkamm, and H. zur Hausen.** 1980. Effect of the diterpene ester TPA on Epstein-Barr virus antigen- and DNA synthesis in producer and nonproducer cell lines. Virology **100**:175-178.
25. **Kintner, C. R., and B. Sugden.** 1979. The structure of the termini of the DNA of Epstein-Barr virus. Cell **17**: 661-671.
26. **Klein, G.** 1979. The relationship of the virus to nasopharyngeal carcinoma, p. 339-350. *In* M. A. Epstein and B. G. Achong (ed.), The Epstein-Barr virus. Springer Verlag, Berlin.
27. **Koller, B., H. Delius, H. Bünemann, and W. Müller.** 1978. The isolation of DNA from agarose gels by electrophoretic elution onto malachite green-polyacrylamide columns. Gene **4**:227-239.
28. **Lee, Y. S., Y. Yajima, and M. Nonoyama.** 1977. Mechanism of infection by Epstein-Barr virus. II. Comparison of viral DNA from HR-1 and superinfected Raji cells by restriction enzymes. Virology **81**:17-24.
29. **Lin, J. C., J. E. Shaw, M. C. Smith, and J. S. Pagano.** 1979. Effect of 12-*O*-tetradecanoyl-phorbol-13-acetate on the replication of Epstein-Barr-virus. I. Characterization of viral DNA. Virology **99**:183-187.
30. **Miller, G., D. Coope, J. Niederman, and J. Pagano.** 1976. Biological properties and viral surface antigens of Burkitt lymphoma- and mononucleosis-derived strains of Epstein-Barr virus released from transformed marmoset cells. J. Virol. **18**:1071-1080.
31. **Miller, G., J. Robinson, L. Heston, and M. Lipman.** 1974. Differences between laboratory strains of Epstein-Barr virus based on immortalization, abortive infection and interference. Proc. Natl. Acad. Sci. U.S.A. **71**:4006-4010.
32. **Miller, G., T. Shope, H. Sisco, D. Stitt, and M. Lipman.** 1972. Epstein-Barr virus: transformation, cytopathic changes, and viral antigens in squirrel monkey and marmoset leukocytes. Proc. Natl. Acad. Sci. U.S.A. **69**: 383-387.
33. **Nilsson, K., G. Klein, W. Henle, and G. Henle.** 1971. The establishment of lymphoblastoid lines from adult and fetal human lymphoid tissue and its dependence on EBV. Int. J. Cancer **8**:443-450.
34. **Pizzo, P. A., I. T. Magrath, S. K. Chattopadhyay, R. J. Biggar, and P. Gerber.** 1978. A new tumour-derived transforming strain of Epstein-Barr virus. Nature (London) **272**:629-631.
35. **Pope, J. H., B. G. Achong, M. A. Epstein, and J. Biddulph.** 1967. Burkitt lymphoma in New Guinea: establishment of a line of lymphoblasts in vitro and description of their fine structure. J. Natl. Cancer Inst. **39**:933-945.
36. **Pope, J. H., M. K. Horne, and W. Scott.** 1968. Transformation of foetal human leukocytes in vitro by filtrates of a human leukemic cell line containing herpes-like virus. Int. J. Cancer. **3**:857-866.
37. **Pope, J. H., M. K. Horne, and W. Scott.** 1969. Identification of the filtrable leukocyte transforming factor of QIMR-WIL cells in herpes-like virus. Int. J. Cancer **4**: 255-260.
38. **Pritchett, R. F., S. D. Hayward, and E. D. Kieff.** 1975. DNA of Epstein-Barr virus. I. Comparative studies of the DNA of Epstein-Barr virus from HR-1 and B95-8 cells: size, structure, and relatedness. J. Virol. **15**:556-569.
39. **Raab-Traub, N., R. Pritchett, and E. Kieff.** 1978. DNA of Epstein-Barr virus. III. Identification of restriction enzymes that contain DNA sequences which differ among strains of Epstein-Barr virus. J. Virol. **27**:388-398.
40. **Rigby, P. W., M. Dieckmann, C. Rhodes, and P. Berg.** 1977. Labeling deoxyribonucleic acid to high specific activity in vitro by nick translation with DNA polymerase I. J. Mol. Biol. **113**:237-251.
41. **Rymo, L., and S. Forsblum.** 1978. Cleavage of Epstein-Barr virus DNA by restriction endonucleases EcoRI, Hind III, and Bam I. Nucleic Acids Res. **5**:1387-1402.
42. **Rymo, L., T. Lindahl, and A. Adams.** 1979. Sites of sequence variability in Epstein-Barr virus DNA from different sources. Proc. Natl. Acad. Sci. U.S.A. **76**:2794-2798.
43. **Shaw, J. E., T. Seebeck, J.-L. H. Li, and J. S. Pagano.** 1977. The Epstein-Barr virus DNA synthesized in superinfected Raji cells. Virology **77**:762-771.
44. **Southern, E. M.** 1975. Detection of specific sequences among DNA fragments separated by gel electrophoresis. J. Mol. Biol. **98**:503-517.
45. **Stüber, D., and H. Bujard.** 1977. Electron microscopy of DNA; determination of absolute molecular weights and linear density. Mol. Gen. Genet. **154**:299-303.
46. **Sugden, B., W. C. Summers, and G. Klein.** 1976. Nucleic acid renaturation and restriction endonuclease cleavage analyses show that the DNAs of a transforming and a nontransforming strain of Epstein-Barr virus share approximately 90% of their nucleotide sequences. J. Virol. **18**:765-775.
47. **Tabak, H. F., and R. A. Flavell.** 1978. A method for the recovery of DNA from agarose gels. Nucleic Acids Res.

5:2321-2332.
48. **Wahl, G. M., M. Stern, and G. R. Stark.** 1979. Efficient transfer of large DNA fragments from agarose gels to diazobenzyloxymethyl-paper and rapid hybridization by using dextran sulfate. Proc. Natl. Acad. Sci. U.S.A. **76:** 3683-3687.
49. **Zur Hausen, H., G. W. Bornkamm, R. Schmidt, and E. Hecker.** 1979. Tumor initiators and promoters in the induction of Epstein-Barr virus. Proc. Natl. Acad. Sci. U.S.A. **76:**782-785.
50. **Zur Hausen, H., F. J. O'Neill, U. K. Freese, and E. Hecker.** 1978. Persisting oncogenic herpesvirus induced by the tumour promoter TPA. Nature (London) **272:**373-375.